Research Square

Preprints are preliminary reports that have not undergone peer review.
They should not be considered conclusive, used to inform clinical practice,
or referenced by the media as validated information.

Isolation and Characterization of a Clinically-Derived Staphylococcus epidermidis HE23: Revealing Its Antibiotic Resistome and Metabolic Potential

Xiaoyan Wang
the First Affiliated Hospital of Anhui Medical University
Qingru Chen
chenqr95@foxmail.com

Anhui Medical University
Wenxin Lin
Anhui Medical University
Yue Gao
Anhui Medical University
Yunyi Qin
Anhui Medical University
Dawei Gao
Lu'an Center for Disease Control and Prevention (CDC)
Maozhen Han
Anhui Medical University
Shenghai Huang
Anhui Medical University

Research Article

Keywords: Staphylococcus epidermidis, neonatal intensive care unit, whole-genome sequencing, antimicrobial resistance, resistome, plasmid

Posted Date: September 20th, 2026

DOI: https://doi.org/10.21203/rs.3.rs-10758913/v1

License: This work is licensed under a Creative Commons Attribution 4.0 International License.
Read Full License

Additional Declarations: No competing interests reported.

Abstract

Neonatal incubators may serve as environmental reservoirs for antimicrobial-resistant bacteria in neonatal intensive care units. In this study, *Staphylococcus epidermidis* HE23 was isolated from a high-touch surface of a neonatal incubator and characterized using whole-genome sequencing, comparative genomics, antimicrobial susceptibility testing, and metabolomic analysis. Hybrid assembly of Illumina and Nanopore sequencing reads generated a complete genome consisting of a circular chromosome (2,542,743 bp) and two plasmids (50,114 bp and 9,031 bp). Genomic analysis identified nine antibiotic resistance genes, including the chromosomal β-lactam resistance determinants *blaZ* and *mecA* and the plasmid-borne mupirocin resistance gene *mupA*. Antimicrobial susceptibility testing further confirmed resistance to multiple antibiotics, including β-lactams and quinolones. Genes associated with resistance to cationic antimicrobial peptides were also identified, suggesting potential mechanisms that may facilitate persistence under antimicrobial pressure. Metabolomic profiling detected several secondary metabolites, including putatively annotated cinobufagin and harmaline. Comparative genomic analysis further revealed conserved and strain-specific genomic features of HE23. The coexistence of chromosomal resistance determinants and plasmid-associated *mupA* highlights the potential of incubator-associated *S. epidermidis* to act as a reservoir of antimicrobial resistance in neonatal intensive care environments. These findings support strengthened microbial surveillance and targeted infection-control strategies for neonatal incubators.

Introduction

Hospital incubators are essential for the specialized care of newborns, particularly premature infants and those with very low birth weights. These devices maintain optimal temperature and humidity, aiding neonatal adaptation to the external environment. However, they also serve as potential reservoirs for microbial proliferation, contributing to healthcare-associated infections (HAIs) in neonates[1]. Pathogens such as methicillin-resistant *Staphylococcus aureus* (MRSA), *Clostridioides difficile*, and *Serratia marcescens* can persist on hospital surfaces and medical equipment[2, 3]. These pathogens can be transmitted through direct contact with contaminated surfaces or indirectly via healthcare personnel [4]. Neonatal incubators, therefore, pose a significant risk of contact-mediated infections, especially for infants with high-risk factors like low birth weight, prematurity, maternal corticosteroid use, mechanical ventilation, and underdeveloped immune systems[5].

Despite extensive research highlighting the importance of environmental disinfection in preventing HAIs, studies show that neonatal incubators remain primary habitats for pathogenic bacteria, such as coagulase-negative *Staphylococci spp*, *Enterococci spp*, and *Bacilli spp*, which are resistant to disinfectants and persist in these environments[6]. This underscores the ongoing challenge in infection control posed by neonatal incubators.

Microorganisms play a crucial role in neonatal health and disease, especially in incubated infants with immature immune systems, making them more susceptible to environmental microorganisms[7, 8].

Microbial exposure can have long-term effects on immune maturation, increasing the risk of future allergic diseases, autoimmune disorders, and other health complications[9]. Microbial infections can also trigger gastrointestinal dysbiosis and skin-related infections, posing significant threats to neonatal well-being. Preterm and low birth weight infants, with underdeveloped immune systems, are particularly vulnerable to pathogenic microorganisms. Microbial exposure can induce abnormal immune responses, hindering normal immune development and increasing the risk of subsequent health issues. Additionally, microorganism infections can disrupt gut microbiota, leading to gastrointestinal problems and impaired nutrient absorption. Skin infections in neonates can result in inflammatory reactions, skin redness, itching, ulceration, and, in severe cases, life-threatening complications such as sepsis[10, 11]. Therefore, effective management and control of microorganism contamination in neonatal environments are paramount to safeguarding their health. Stricter protective measures are essential for preterm and low-birth weight infants to minimize exposure to pathogenic microorganisms and mitigate the risks associated with their immature immune systems. Emphasizing microbial management and environmental cleanliness will help reduce infection risks and promote healthy development and growth.

Considering the complex and diverse hospital environment where various microorganisms coexist, the potential microorganism threats within incubators pose significant concerns, especially for vulnerable neonatal populations, we isolated a bacterial strain from an incubator at the Fourth Affiliated Hospital of Anhui Medical University and subsequently identified the species through 16S rRNA gene sequencing. Combined with the findings from whole-genome sequencing, the strain was conclusively characterized as *S. epidermidis*. *S. epidermidis*, a common Gram-positive bacterium, typically exists in the form of cocci, aerobic and facultative anaerobic bacteria thriving in warm and nutrient-rich environments. Within the human body, *S. epidermidis* is widely present on the skin surface, sweat glands, and sebaceous glands. As a constituent of the normal microbiota, *S. epidermidis* plays a crucial role in maintaining skin health and immune function. *S. epidermidis* is a group of coagulase-negative staphylococci (CoNS), commonly found in the environment and extensively present on the human skin surface. Although *S. epidermidis* has historically been considered a harmless commensal bacterium of the human skin microbiota, a growing body of research suggests that it is a clinically important opportunistic pathogen. [12–15]. *S. epidermidis* has been identified as a primary pathogenic factor in nosocomial surgical device-related infections[16, 17]. Furthermore, numerous strains of *S. epidermidis* carry antibiotic-resistance genes and genes involved in biofilm formation, posing challenges to clinical treatment to some extent[18, 19]. Of particular note is the association between *S. epidermidis* and neonatal sepsis. Clinical studies indicate the presence of *S. epidermidis* in the bodies of some neonatal sepsis patients. Research also suggests that *S. epidermidis* may trigger skin infections in neonates, manifesting as symptoms such as skin redness, pain, and pustules. In severe cases, these infections may disseminate into the bloodstream, causing sepsis and even leading to serious complications such as skin tissue necrosis, posing a threat to the health of neonates[20]. It is noteworthy that studies have shown that *S. epidermidis* is not simply pathogenic or nonpathogenic, but that there is a continuum of pathogenicity influenced by strain-specific genomic and phenotypic variation. Although *S. epidermidis* is a normal component of the human skin microbiota, under certain circumstances, it may incite infection.

Particularly in the case of neonates, whose immune systems are not yet fully developed, they are more susceptible to allergies or infections after exposure to bacteria in environments such as incubators. As a common member of the skin microbiota, *S. epidermidis* may serve as a potential source of infection and disease at such times. Hence, early prevention and identification are crucial.

We employed multi-omics approaches to characterize this bacterial strain, including whole-genome sequencing data analysis, comparative genomics, and metabolomics. Our study delineates the features of *S. epidermidis* isolated from neonatal incubators, providing novel insights into the risks faced by vulnerable infants in this understudied yet clinically critical environment, as well as the genomic adaptations of healthcare-associated strains.

Materials and methods

Samples collection

Clinical samples (n = 4) were collected from neonatal incubators in the NICU at the First Affiliated Hospital of Anhui Medical University between 2:00–7:00 on August 14. All incubators had been in continuous use for 14 days with twice-daily disinfection (0.5% hydrogen peroxide spray + 30-min UV irradiation). Environmental parameters during sampling were recorded as mean temperature 36.5 ± 0.3°C and relative humidity 60 ± 5%. Sterile swabs were used to wipe 10×10 cm areas of inner walls and immediately inoculated into lysogeny broth (LB) broth (10 g/L tryptone, 5 g/L yeast extract, 10 g/L NaCl, pH 7.2). Cultures were incubated at 36°C with 5% CO_2 and orbital shaking (100 rpm) for 24 hours, followed by serial plating on LB agar for pure culture isolation. Strain purity was validated by: (1) morphological uniformity of colonies; (2) amplification of the 16S rRNA gene of the strain by the universal primers 27F (5'-AGAGAGTTTGATCCTGGCTCAG-3') and 1492R (5'-GGTTACCTTGTTACGACTT-3') under the following PCR conditions: initial denaturation at 94°C for 5 minutes; 35 cycles (94°C for 30 seconds, 55°C for 30 seconds, 72°C for 30 seconds); and final extension at 72°C for 5 minutes. Purified PCR products were sequenced in both directions and compared using BLASTn against NCBI RefSeq core_nt database.

Scanning electron microscopy sample preparation and imaging analysis

The bacterial samples were cultured in LB medium at 36°C with 5% CO_2 (100 rpm, 48 h), then centrifuged (3,000 ×g, 5 min). Pellets were fixed with 1% OsO_4 in 0.1 M PBS (4°C, 1 h), washed with PBS, and dehydrated through an ethanol series (30–100%). After critical point drying (Quorum K850), samples were sputter-coated with 10 nm Au/Pd (Hitachi MC1000) and imaged by SEM (Hitachi SU8100, 5–15 kV, 5,000–50,000×).

Genomic DNA extraction and sequencing

S. epidermidis HE23 was cultured overnight on LB agar at 37°C. A single colony was inoculated into 100 mL LB broth and grown to logarithmic phase (37°C, 100 rpm). Cells were pelleted by centrifugation (12,000 × g, 10 min, 4°C), washed with sterile water, and genomic DNA was extracted using a magnetic bead-based bacterial DNA kit (T07-100, China). DNA quality was verified spectrophotometrically (A260/A280 = 1.8–2.0).

Whole-genome sequencing was performed using Illumina NovaSeq6000 with NovaSeq XP kit (version 2) (paired-end, 2 × 150 bp) and Oxford Nanopore PromethION platforms. For Illumina libraries, DNA was fragmented (~ 400 bp), adapter-ligated (NEXTFLEX Rapid DNA-Seq Kit, version2.0), and size-selected via agarose gel electrophoresis. Nanopore libraries were prepared using the SQK-LSK109 kit, including DNA repair, end-polishing, and adapter ligation. Illumina sequencing employed cyclic reversible termination chemistry with fluorescently labeled dNTPs. Nanopore libraries were loaded onto R9.4.1 Flow Cells for real-time single-molecule sequencing via current signal detection.

Genome quality control, assembly

Raw Illumina sequencing data were processed using fastp (v0.23.0) [21] for quality trimming, including removal of low-quality reads (Phred score < Q15), reads with excessive N content (> 10%), and adapter sequences. Nanopore raw sequencing data, initially stored as binary fast5 files containing raw electrical signals, were base-called and converted to fastq format. Reads with an average Q score > 7 were retained for downstream analysis. Quality control for both platforms was performed with default parameters: minimum read length of 15 bp, Phred quality threshold ≥ Q15, and sequence complexity threshold of 30 (complexity_threshold = 30). Adapter trimming for Nanopore reads was performed with Porechop v0.2.4 using the --discard_middle parameter.

Hybrid assembly of quality-controlled Illumina short reads (2×150 bp) and Nanopore long reads was performed using Unicycler (v0.4.8) [22] under default parameters, configured in hybrid mode (--mode bold) to integrate SPAdes-based short-read assembly (k-mer range: 21–127) with long-read scaffolding (minimum overlap identity: 95%, --min_identity 95). Contigs shorter than 200 bp (--min_fasta_length 200) and low-coverage regions (< 0.25× depth, --depth_filter 0.25×) were automatically filtered. The resulting draft genome was polished iteratively using Pilon v1.22 with Illumina short reads mapped via Bowtie2 (minimum base quality: Q20) over three cycles to correct base errors, resolve indels, and fill gaps (--fix bases, gaps). Assembly quality was assessed using QUAST (v5.2.0)[23]

Functional annotations

The assembled genomic data were annotated using Prokka (version 1.14.6)[24]. Prodigal(version 2.6.2) [25] was employed for gene prediction across bacterial genomes. Sequences relevant to virulence factor genes, antibiotic resistance genes, carbohydrate enzyme genes, and phosphorus cycling genes were identified with Diamond[26] using the Virulence Factor Database (VFDB)[27], ARG database (version 2.0)

[28], CAZymes (version 3.2.1), and PCyCDB (version 1.1), respectively. METABOLIC (version 4.0)[29] was utilized for analyzing genes implicated in nitrogen and sulfur cycling within the genome.

Genome-based metabolic analysis

To systematically characterize the metabolic pathways of *S. epidermidis* HE23, we performed genome-scale functional annotation and pathway reconstruction. First, protein-coding genes predicted from the genome assembly were functionally annotated using KofamScan (version1.3.0; GitHub: https://github.com/takaram/kofam_scan; accessed April 3, 2024). This tool aligns protein sequences against the KEGG Orthology (KO) entries in the Kyoto Encyclopedia of Genes and Genomes (KEGG) database through hidden Markov models (HMMs), with thresholds set at e-value < 1e − 5 and score above KO-specific cutoffs. The raw output was converted into standardized KO annotation tables and metabolic enzyme gene lists using the built-in kofamscan2table.py script. For metabolic network elucidation, the annotated data were submitted to the KEGG Mapper platform (https://www.genome.jp/kegg/mapper; accessed April 3, 2024) [30]. The "Reconstruct Pathway" module was employed for automated pathway mapping and visualization. Finally, interactive KEGG pathway network diagrams were generated in RStudio (v2023.12.0) using the ggplot2 and igraph packages. Nodes represented metabolic pathways (classified by KO hierarchy), and edge weights indicated functional gene connectivity between pathways, providing a global perspective on the core metabolic features and potential crosstalk mechanisms of *S. epidermidis* HE23.

Untargeted metabolomics analysis

S. epidermidis HE23 was inoculated into LB broth (10 g/L tryptone, 5 g/L yeast extract, 10 g/L NaCl) and cultured aerobically at 37°C with 100 rpm shaking for 72 hours. Three biological replicates and three blank controls (LB broth only) were included. Bacterial cells at mid-log phase were harvested by centrifugation (4,000 ×g, 10 min, 4°C), followed by metabolite extraction using ice-cold methanol/water (80:20, v/v). The mixture was vortexed for 30 sec, ultrasonicated on ice for 10 min, and centrifuged (12,000 ×g, 15 min, 4°C) to collect the supernatant for LC-MS analysis.

Chromatographic separation was performed on a Thermo Dionex Ultimate 3000 UHPLC system equipped with an ACQUITY UPLC HSS T3 column (100 mm × 2.1 mm, 1.8 μm; Waters, USA). The mobile phases consisted of (A) 0.1% formic acid in water-acetonitrile (95:5, v/v) and (B) 0.1% formic acid in acetonitrile-isopropanol-water (47.5:47.5:5, v/v/v). The gradient elution program was set as follows: 0–0.5 min, 40% B to 50% B (linear); 0.5–3.5 min, 50% B to 55% B (linear); 3.5–6.0 min, 55% B to 70% B (linear); 6.0–7.0 min, 70% B to 100% B (linear), held at 100% B until 8.0 min. The column temperature was maintained at 40°C with an injection volume of 3 μL. Mass spectrometry was conducted on a Thermo Scientific UHPLC-Q Exactive HF-X Orbitrap system equipped with an electrospray ionization (ESI) source operated in separate positive and negative ion modes. Ionization parameters included a spray voltage of ± 3.5 kV, capillary temperature of 325°C, sheath gas flow rate of 50 arb, and auxiliary gas flow rate of 13 arb. Full-scan spectra were acquired over m/z 70–1050 with a resolution of 60,000 (@ m/z 200).

Raw MS data were processed using Progenesis QI v3.0 (Waters Corporation, USA) for peak picking, retention time alignment, and feature matrix generation (containing m/z, RT, and intensity). Metabolite annotation was performed against the KEGG (Kyoto Encyclopedia of Genes and Genomes) databases with thresholds of MS/MS match score > 80% and mass error < 5 ppm. Multivariate statistical analysis (e.g., PLS-DA) was implemented in SIMCA 14.1, while pathway enrichment analysis was conducted via MetaboAnalyst (version 6.0, https://www.metaboanalyst.ca/, accessed April 18, 2024). Differential metabolites were screened based on the following criteria: (1) absolute fold change (upregulated: FC ≥ 2; downregulated: FC ≤ 0.5), (2) variable importance in projection (VIP) scores ≥ 1 derived from orthogonal partial least squares-discriminant analysis (OPLS-DA), and (3) statistical significance confirmed by Student's t-test ($p < 0.05$).

Secondary metabolite gene cluster analysis using antiSMASH

In this investigation, we analyzed the bacterial genomic data using the web tool antiSMASH (version 7.1.0)[31] in conjunction with the antiSMASH database. After the submission of genomic data, antiSMASH embarked on the detection and prognosis of potential biosynthetic pathways, non-coding RNAs, secondary metabolic gene clusters, and other pertinent secondary metabolite-associated genes. Notably, the tool undertakes genome annotation, gene prediction, and enzyme coding prediction among other operations.

Phylogenetic trees and MLST typing

The 16S rRNA sequences were extracted from the bacterial genomes using Barrnap (version 0.9), and taxonomic identification was performed through BLAST analysis against the NCBI RefSeq core_nt database. The top 49 16S rRNA sequences exhibiting the highest similarity to the query sequences were compiled from NCBI's rRNA database, enriching the dataset for comparative purposes. Finally, maximum likelihood tree construction was performed using MEGA (version12) software, with the model configuration set to the K2 + G + I combination (i.e., the Model/Method parameter was set to the Kimura 2-parameter model, and the Rates among Sites parameter was set to the Gamma Distributed with Invariant Sites mode). Additionally, to achieve precise strain classification within the *S. epidermidis* population structure, conventional MLST and rMLST analyses were performed on the assembled whole-genome sequence of HE23 using the PubMLST platform (https://pubmlst.org/).

Antibiotic susceptibility testing

S. epidermidis HE23 was adjusted to a standardized inoculum density of 0.5 McFarland (~ 1.5 × 10^8 CFU/mL) using sterile saline, inoculated uniformly on LB agar plates, and incubated at 37°C. After incubation, the growth inhibition zones around each antibiotic disc were observed and measured using the VITEK2 system (BioMérieux, France) with the Gram-positive cocci susceptibility testing panel. Results were interpreted according to CLSI (2023) breakpoints for coagulase-negative staphylococci.

Comparative genomic analysis

To evaluate the phylogenetic relationship and genomic features of *S. epidermidis* HE23, eight reference genomes were retrieved from NCBI based on taxonomic classification and completeness. OrthoANI values between *S. epidermidis* HE23 and the reference strains were calculated using OAT (version 0.93.10), employing a bidirectional best-hit algorithm to identify orthologous clusters. Genomic synteny between *S. epidermidis* HE23 and *S. epidermidis NBRC 100911* (highest ANI: 99.88%) was visualized via BRIG (version 0.5). Orthologous gene clusters were analyzed with OrthoVenn3 (E-value ≤1e − 5, identity ≥ 50%, https://orthovenn3.bioinfotoolkits.net), generating Venn diagrams and bar plots. Visualization parameters were standardized across tools to ensure consistency.

Results

Cell culture morphological characteristics

The strain exhibited distinct morphologies in solid and liquid cultures. Colonies on nutrient agar formed discrete circular structures (mean 2 mm diameter) with smooth, milky-white surfaces, central protrusions, and peripheral depressions after 24 hours (Fig. 1A). Liquid cultures showed uniform turbidity under shaking, indicating stable planktonic growth, with minor sedimentation after > 48 hours. Scanning electron microscopy further resolved the coccoid cellular morphology, with cells exhibiting typical staphylococcal clustering and intact surface structures under high magnification (Fig. 1B).

Genomic characterization and phylogenetic analysis

The total size of the *S. epidermidis* genome is 2,601,888 base pairs, comprising three contigs, with the largest contig reaching 2,542,743 base pairs. The N50 and N90 values are 2,542,743 base pairs, with an average coverage depth of 545-fold, which achieves a complete coverage rate of 100% and a successful mapping rate of 99.93%. The overall GC content is 32.18%. The genome of this organism was analyzed, and it was found that it has a chromosome of 2,542,743 base pairs and two plasmids (Plasmid 1: 50,114 bp; Plasmid 2: 9,031 bp). A total of 2,447 protein-coding genes were predicted, with 1,588 genes (64.9%) annotated as functional genes and 859 genes (35.1%) annotated as hypothetical genes. Additionally, there are 79 RNA genes, including 63 tRNA and 16 rRNA (5 16S rRNA, 5 23S rRNA, and 6 5S rRNA genes, Table 1)

Table 1
Characteristics of the draft genomes of *S. epidermidis strain HE23.*

Parameter	Numbers
Genome size (bp)	2,542,743
G + C content (%)	32.18
No. of contigs	3
The largest contig (bp)	2,542,743
The shortest contig (bp)	9,031
N50	2,542,743
L50	1
Protein-coding sequences	2,447
Hypothetical proteins	859
Functional proteins	1,588
rRNA	16
tRNA	63
CRISPRs candidates	4

According to the BLAST analysis of the 16S rRNA sequence against NCBI, the bacterium shows a 100% match with *S. epidermidis*, a 100% coverage, and an expected value of 0.0, indicating the reliability of the result. It is preliminary concluded that the bacterium belongs to the species of *S. epidermidis*. Following this, a phylogenetic tree was constructed based on the 16S rRNA sequences to infer the evolutionary relationships among microbes by comparing the differences in this sequence. During the tree-building process, an evolutionary analysis and the construction of the phylogenetic tree were conducted using the 49 most similar 16S rRNA sequence data to the target sequence through the maximum likelihood method. The results of the evolutionary tree show that two clades of *S. epidermidis* strains (Fussel and NBRC 100911) are clustered in the same branch as HE23, indicating a close evolutionary relationship. This finding further validated the species identification established through 16S rRNA sequence analysis, confirming the isolate as *S. epidermidis*. (Fig. 2). MLST analysis via PubMLST assigned HE23 to a novel sequence type (ST-HE23; 6/7 loci match with ST-5, mismatch at arcC), rMLST confirmed species identity (rST: 313845).

Functional annotation

Through comparative analysis with the antibiotic resistance gene database, we have identified 9 genes on the bacterial chromosome with potential antibiotic resistance, namely *mecA*, *gyrA*, *mgrA*, *norA*, *dfrC*,

blaZ, *sdrM*, *sepA*, and *norC* (Fig. 3A). These genes may play pivotal roles in bacterial resistance to antibiotics, involving modifications of targets for different antibiotics and drug metabolism mechanisms. Apart from the genes on the bacterial chromosome, we also detected an antibiotic-related gene named *mupA* on a plasmid (Fig. 3B). The presence of *mupA* could potentially provide bacteria with additional mechanisms for antibiotic resistance, thereby augmenting bacterial resistance to antibiotics.

Furthermore, these genes were also compared with the virulence factor database, revealing 13 genes related to virulence on the bacterial chromosome, including *atl*, *ebh*, *sdrE*, and others (Fig. 3A), which are associated with bacterial virulence factors and pathogenicity. Moreover, an analysis of genes related to nitrogen, phosphorus, and sulfur cycles in the bacterial genome was conducted. These genes are all located on the bacterial chromosome, including a nitrogen cycle-related gene (*narG*), a sulfur cycle-related gene (*sat*), and two phosphorus cycle genes (*gntK*, *dut*), participating in bacterial nutrient metabolism processes and utilization of nitrogen, phosphorus, and sulfur resources in the environment.

Metabolomics analysis

KEGG pathway analysis of the *S. epidermidis* HE23 genome revealed distinct functional enrichments associated with its adaptation to clinical environments (Fig. 4A, 4B). The Genetic Information Processing category accounted for 12–15% of annotated genes (184 genes). Key pathways within this category included Ribosome (55 genes) and Aminoacyl-tRNA biosynthesis (25 genes), which are critical for maintaining translational efficiency under stress conditions such as antibiotic exposure.

The Environmental Information Processing category (163 genes) was dominated by Two-component systems (62 genes) and ABC transporters (58 genes), indicating enhanced capabilities for environmental signal perception and nutrient acquisition. These systems are likely essential for surviving nutrient-limited hospital environments and resisting antimicrobial pressures. In the Metabolism category (1,896 genes), the prominence of Metabolic pathways (422 genes) and Biosynthesis of secondary metabolites (208 genes) suggests metabolic versatility, enabling utilization of diverse substrates and production of stress-responsive compounds. Notably, the Human Diseases category (88 genes) included a high number of genes linked to antibiotic resistance, such as β-lactam resistance (13 genes) and Cationic antimicrobial peptide (CAMP) resistance (10 genes), consistent with the strain's clinical origin. Additionally, the Cellular Processes category (62 genes) featured Quorum sensing (35 genes) and biofilm-related pathways, traits previously associated with persistent medical device infections(*S1*).

These genomic features collectively highlight *S. epidermidis* HE23's adaptation to hospital niches through enhanced translational capacity, stress-responsive signaling, and resistance mechanisms, aligning with its role as a nosocomial pathogen.

Metabolomic analysis of *S. epidermidis* HE23 revealed distinct metabolic profiles and pathway enrichments aligned with its genomic adaptations (Fig. 5). The Metabolism category dominated the KEGG pathway distribution, with "Global and overview maps" (214 genes) and "Amino acid metabolism" (88 genes) representing the most gene-enriched pathways (Fig. 5A). Pathway enrichment analysis

highlighted significant associations with pyruvate metabolism, glycerolipid metabolism, and glutathione metabolism (Fig. 5B), pathways critical for energy homeostasis and oxidative stress response. For instance, "Pyruvate metabolism" (enrichment ratio = 4.0, p = 0.000001) aligns with the strain's need for rapid substrate utilization in nutrient-limited environments. Key secondary metabolite biosynthesis pathways, such as "Biosynthesis of other secondary metabolites" (33 genes), further underscored the strain's metabolic versatility. Among differentially expressed metabolites, 15 were significantly upregulated and 32 downregulated in bacterial cultures compared to sterile LB medium controls (Fig. 5C). Among the up-regulated differential metabolites, some substances of interest were found (Fig. 5D), such as harmaline and cinobufagin. Harmaline is a derivative of β-hydroxy-2-phenylethylamine, which is common in certain plants, especially those belonging to the family of Rhamnaceae. It has been found to have potent monoamine oxidase inhibitor activity, which means that it may affect the metabolism and release of neurotransmitters and thus have an effect on the central nervous system. It has been shown that Akkermansia muciniphila secretes harmaline and has a mitigating effect on severe fever with thrombocytopenia syndrome virus infection[30, 32]. Another metabolite of interest is cinobufagin, a toxic alkaloid found mainly in the skin of toads. It is often used as one of the ingredients in traditional Chinese medicine and is thought to have anticancer, anti-inflammatory, and blood circulation-enhancing properties. However, cinobufagin is also highly toxic, and overdose may lead to poisoning or even death[33, 34]. In addition, the up-regulated metabolite identified the β-lactamase inhibitor, tazobactam, which irreversibly binds to β-lactamase and blocks its ability to hydrolyze β-lactam antibiotics (e.g., penicillins and cephalosporins).

These findings collectively illustrate *S. epidermidis* HE23's metabolic adaptability, integrating genomic resilience (e.g., antibiotic resistance) with dynamic metabolite production to thrive in clinical settings.

Carbohydrate enzyme analysis

The genomic characterization of *S. epidermidis* HE23 revealed 489 putative CAZymes, with glycoside hydrolases (GHs, 208 genes) and glycosyltransferases (GTs, 194 genes) constituting the predominant functional classes (Fig. 6A). Notably, the GH13 family, a group frequently associated with starch/glycogen metabolism in Staphylococci accounted for the largest subset of GHs. Similarly[35], GT2 and GT4 families dominated the GT class, collectively representing 61% of GTs (Fig. 6B). These families are critical for synthesizing extracellular polysaccharides (EPS), which serve as structural scaffolds in bacterial biofilms[36]. The observed enrichment of GH13, GT2, and GT4 aligns with the canonical CAZyme repertoire of *S. epidermidis* but highlights strain-specific expansions in EPS-related machinery. Such genomic features may facilitate biofilm-mediated colonization on medical devices, as EPS production is a well-documented virulence determinant in nosocomial infections.

Secondary metabolite gene clusters

We performed secondary metabolite analysis on the genomic data, revealing information such as gene cluster types, positional ranges, and similarity to known clusters in different regions (Table 2). In Region

1, there are multiple types of gene clusters, such as opine-like-metallophore, NRPS, T3PKS, NI-siderophore, each potentially encoding various categories of secondary metabolites, such as metal carriers, sugars, and polyketides. Some of these exhibit high similarity (100%) to known metabolic clusters, such as staphylopine and staphyloferrin A, both compounds produced by *Staphylococcus aureus*, playing vital roles in metal ion capture and utilization, as well as serving as iron carriers, crucial for the survival of *S. aureus*. Others display lower similarity, such as micrococcin P1, chejuenolide A/chejuenolide B, and berninamycin. In Region 3, a RiPP-like gene cluster was discovered, potentially encoding secondary metabolites resembling RiPPs (Ribosomally synthesized and post-translationally modified peptides).

Table 2
Biosynthetic gene clusters of *S. epidermidis strain HE23*.

Region	Location (nucleotide to nucleotide)	Type	Most similar known cluster	Similarity (%)
Region 1.1	144367–166467	opine-like-metallophore	Staphylopine	100
Region 1.2	174260–221423	NRPS	-	-
Region 1.3	302917–326844	saccharide	-	-
Region 1.4	394604–435770	T3PKS	-	-
Region 1.5	478040–507739	saccharide	-	-
Region 1.6	577898–605951	saccharide	-	-
Region 1.7	729556–762548	NI-siderophor	staphyloferrin A	100
Region 1.8	874708–895416	cyclic-lactone-autoinducer	-	-
Region 1.9	1420091–1448978	saccharide	micrococcin P1	8
Region 1.10	1923175–1945372	fatty_acid	chejuenolide A/chejuenolide B	7
Region 1.11	2295498–2337447	saccharide	berninamycin K/berninamycin J/berninamycin A/berninamycin B	22
Region 1.12	2428671–2455772	saccharide		
Region 1.13	2487008–2522053	saccharide		
Region 3.1	1-9031	RiPP-like	-	-

Comparative genome analysis

To analyze the genetic characteristics of *S. epidermidis* HE23 and its evolutionary relationships with other clinical strains, we first assessed the genomic similarity between *S. epidermidis* HE23 and eight reference strains using Average Nucleotide Identity (ANI) analysis. The phylogenetic heatmap based on OrthoANI values revealed that the ANI values between *S. epidermidis* HE23 and other strains ranged

from 99.33% to 99.88%, with the highest genetic similarity observed with *S. epidermidis NBRC 100911* (Fig. 7A). This indicates a highly conserved core genome between these two strains. Further collinearity analysis using the BRIG tool demonstrated that *S. epidermidis* HE23 and the reference strain *S. epidermidis ATCC 14990* exhibited a high degree of linear conservation in the main chromosomal backbone regions (Fig. 7B). However, significant genomic rearrangements and insertion-deletion variations were evident in localized regions, suggesting that *S. epidermidis* HE23 may have acquired unique genetic elements through horizontal gene transfer. Additionally, we performed a proteomics comparison of *S. epidermidis* HE23 with four other *S. epidermidis* strains (ATCC 14990, B1272014, B1276912, and NBRC 100911). OrthoVenn3 analysis identified a total of 2,095 shared protein clusters, encompassing core metabolic pathways, DNA repair mechanisms, and cell wall synthesis. Furthermore, each strain harbored unique protein clusters: *S. epidermidis* HE23 contained 15 specific clusters, while ATCC 14990, B1272014, B1276912, and NBRC 100911 possessed 21, 24, 31, and 41 unique clusters, respectively (Fig. 7C, 7D). Quantification of cluster distribution using bar charts showed that 29 clusters were strain-specific, 120 clusters were shared by two strains, 54 clusters by three strains, 3 clusters by four strains, and only one cluster was fully conserved across all five strains (Fig. 7E).

Antibiotic susceptibility testing

The antibiotic susceptibility testing revealed that the strain exhibited resistance to oxacillin (MIC ≥ 4 μg/mL) and penicillin G (MIC ≥ 0.5 μg/mL), consistent with *mecA*-mediated β-lactam resistance, and to levofloxacin (MIC = 4 μg/mL). Intermediate susceptibility was observed for moxifloxacin (MIC = 1 μg/mL) and ciprofloxacin (MIC = 2 μg/mL). Full susceptibility was demonstrated to all other tested agents. (Table 3).

Table 3
Information on antibiotic resistance and related parameters.

No	Antibiotic	MIC	Drug sensitivity results	Result Flag
1	Oxacillin	>=4	resistant	R
2	Penicillin G	>=0.5	resistant	R
3	Erythromycin	0.5	sensitive	S
4	Clindamycin	<=0.25	sensitive	S
5	Levofloxacin	4	resistant	R
6	Moxifloxacin	1	intermediate	I
7	Quinupristin/dalfopristin	0.5	sensitive	S
8	Ciprofloxacin	2	intermediate	I
9	Furantoin	<=16	sensitive	S
10	Compound Xinnuomin	<=10	sensitive	S
11	Linazolamide	1	sensitive	S
12	Rifampicin	<=0.5	sensitive	S
13	Tetracycline	4	sensitive	S
14	Tigecycline	<=0.12	sensitive	S
15	Erythromycin	1	sensitive	S

Discussion

Staphylococcus epidermidis, a common microbe found on human skin, thrives on both skin and mucosal surfaces. It derives nutrients from substances secreted by hair follicles and sebaceous glands[37]. This bacterium typically establishes a symbiotic relationship with humans, providing the host with a degree of protection. Through spatial occupancy and resource competition, *S. epidermidis* inhibits the growth of other pathogenic organisms, thereby reducing the risk of infection. Additionally, it enhances its defensive mechanisms by producing various antimicrobial substances, such as antimicrobial peptides, acidic compounds, and enzymes, which serve as barriers against bacterial, fungal, and viral infections[38]. These defense mechanisms contribute to the maintenance of skin health. Despite being a part of the normal microbial flora, *S. epidermidis* can become opportunistic and potentially pathogenic under certain conditions, such as in hospital environments or when the host's immune system is compromised, leading to infections[39].

S. epidermidis is often implicated in infections associated with indwelling surgical devices, such as artificial heart valves, catheters, and intubation tubes. It possesses the capacity to form biofilms,

affording the bacteria the ability to adhere to medical device surfaces and resist antibiotics. Once introduced into the body and allowed to proliferate around the indwelling surgical apparatus, these bacteria can incite infection. The occurrence of infections related to indwelling surgical devices can lead to severe complications, particularly in vulnerable populations such as neonates with weakened immune systems. For these patients, infections may rapidly disseminate, leading to systemic infection and even life-threatening outcomes[40, 41].

In addition, recent studies have revealed an association between *S. epidermidis* and late-onset sepsis in neonates. Late-onset sepsis (LOS) refers to infections and sepsis occurring between 72 hours and 28 days after birth, distinct from early-onset sepsis (EOS) which manifests within the initial 48 hours postpartum[42, 43]. Late-onset sepsis stands as a major contributor to neonatal mortality, particularly affecting premature and low birth weight infants. The etiology of LOS is diverse, with bacteria, notably Gram-negative bacteria, being the most prevalent pathogens[44, 45]. *S. epidermidis* is a common pathogen implicated in LOS. Despite its typical commensal role on human surfaces, this bacterium may emerge as a significant pathogen in hospital settings, especially neonatal intensive care units, where it contributes to late-onset sepsis in neonates. Given the incomplete development of the neonatal immune system and the invasive procedures such as intubation and venous catheterization associated with hospitalization, these factors predispose *S. epidermidis* to enter the bloodstream of neonates from the skin surface, triggering sepsis[46–48].

S. epidermidis exhibits remarkable biofilm formation capability and a high prevalence of antibiotic resistance, serving as a reservoir for numerous antibiotic-resistant genes. Studies have revealed the inter-group transfer of antibiotic resistance genes, such as those for erythromycin, tetracycline, and chloramphenicol, mediated by specific bacteriophages within the *S. epidermidis* population, along with bacteriophage-induced chromosomal island transfer. These genes can also be disseminated within the *Staphylococcus* population through horizontal gene transfer mechanisms such as transduction[49]. In our research, we conducted comparative analyses using the KEGG database and scrutinized the metabolic pathway-associated genes within the bacterial genome. Regarding genes implicated in human diseases, this strain may pose a potential threat. Primarily, the bacterial genome harbors genes associated with antibiotic resistance, conferring resistance to β-lactam antibiotics. The β-lactam antibiotics encompass a specific β-lactam ring within their structure, crucial for their antibacterial activity, commonly exhibiting efficacy against Gram-positive bacteria and some Gram-negative bacteria, constituting a widely utilized class of antibiotics in clinical practice for bacterial infection treatment[50]. Among the antibiotic resistance genes identified, the *mecA* gene is closely associated with β-lactam antibiotic resistance. It encodes an altered penicillin-binding protein, PBP2a, which has a low affinity for β-lactam antibiotics. This results in resistance through target modification, preventing the antibiotics from effectively inhibiting cell wall synthesis[51, 52]. In contrast, the *blaZ* gene encodes a β-lactamase, which enzymatically degrades these antibiotics, thereby reducing their efficacy and shielding bacteria from their inhibition[53].Notably, LC-MS/MS metabolomic profiling detected a metabolite matching tazobactam in this strain, it's a synthetic β-lactamase inhibitor, irreversibly inactivates β-lactamases and potentiates β-lactam antibiotics[54]. While bacterial biosynthesis of tazobactam itself is unprecedented,

some microbes produce analogous inhibitors[55]. *S. epidermidis* HE23 may exploit such a strategy to inhibit competing β-lactamase producers in its niche, while maintaining intrinsic resistance via *mecA*-encoded PBP2a modification. However, the low MS/MS spectral match score (0 vs. theoretical 37.2) necessitates further validation. If confirmed, this could indicate a competitive ecological advantage in clinical environments. Furthermore, the *gyrA* gene is a critical player in quinolone antibiotic resistance. This gene encodes an enzyme involved in bacterial DNA synthesis, mutations of which may confer resistance to quinolone antibiotics. The results of the antimicrobial sensitivity testing also confirmed the bacterium's resistance to β-lactam antibiotics (such as benzylpenicillin) and quinolone antibiotics (such as levofloxacin)[56, 57]. In this study, in addition to identifying genes associated with antibiotic resistance potential on the bacterial chromosome, we also discovered an antibiotic-related gene named *mupA* within the bacterial plasmid. The *mupA* gene may be involved in multiple mechanisms of antibiotic resistance. It likely encodes a channel protein capable of influencing the entry of antibiotics into bacterial cells, thereby preventing antibiotics from accumulating sufficiently within the bacteria to exert bactericidal effects. Furthermore, the *mupA* gene may also encode an enzyme capable of degrading specific antibiotics, thus enhancing the bacteria's resistance to this class of antibiotics[58]. The presence of the *mupA* gene in the plasmid provides bacteria with another important mechanism of resistance, which could have significant implications for our understanding of bacterial resistance mechanisms and the development of new antibiotics. This resistance trait increases the risk of difficulty in effectively eradicating infections during treatment. Antibiotic resistance poses a significant challenge in the medical field, especially considering the frequent use of β-lactam antibiotics for infection treatment.

Furthermore, the genomic repertoire of this strain encompasses certain genes or pathways associated with antimicrobial peptide resistance, endowing the strain with resilience against cationic antimicrobial peptides. Antimicrobial peptides (AMPs) stand as one of the most promising alternatives in the quest for new therapies against microbial resistance mechanisms towards conventional antibiotics. Among various types of AMPs, cationic antimicrobial peptides exhibit prominent characteristics, serving as vital constituents in the defense against microbial assaults, constituting a pivotal component of the human innate immune system, crucial for warding off pathogenic microorganisms [37]. Studies have elucidated evolutionary adaptations in certain bacteria, such as MRSA, which may reduce susceptibility to certain cationic peptides by modulating the teichoic acid content on their surface[59]. Additionally, some bacteria mitigate the affinity to cationic antimicrobial peptides by substituting cationic molecules for anionic surface components. The emergence of these resistance mechanisms complicates the treatment of bacterial infections, underscoring the imperative of researching and comprehending these mechanisms to develop novel antimicrobial strategies to confront the challenge posed by resistant bacteria[60]. It is plausible that this strain may have developed resistance to these antimicrobial peptides, potentially facilitating its survival and proliferation in hosts or environments, heightening the risk of pathogenicity in humans. This underscores the necessity for further investigation into its resistance mechanisms, along with heightened vigilance concerning resistant bacteria within hospital environments.

In recent years, research on the antibiotic resistance of *S. epidermidis* has increasingly become a focal point in the global medical community. Clinical observations indicate that *S. epidermidis* isolated from hospital environments almost always exhibit resistance to multiple antibiotics, with methicillin-resistant strains being predominant[61]. It is noteworthy that the proportion of methicillin-resistant *S. epidermidis* (MRSE) clinically isolated in China has sharply risen in recent years, becoming one of the primary pathogens causing clinical infections[62]. The resistance of *S. epidermidis* is primarily transmitted through plasmid-encoded resistance genes, which confer multi-drug resistance in clinical settings. Not only do they exhibit strong resistance to common antibiotics such as penicillin, ampicillin, and cephalothin, but they also demonstrate resistance to commonly used therapeutic drugs like vancomycin, further exacerbating the demand for effective treatment methods. While some antibiotics are still effective in treating infections caused by *S. epidermidis*, the increasing misuse of antibiotics, exemplified by the emergence of vancomycin-resistant strains, may gradually diminish their efficacy. Unlike *S. aureus*, the pathogenic mechanism of *S. epidermidis* mainly involves evading the host immune system by forming biofilms, thus establishing long-term infections within hosts. The formation of these biofilms is closely associated with the extracellular matrix secreted by bacteria and the multilayered structures they collectively form, possessing strong adhesion and resistance properties. This enables *S. epidermidis* to cause infections on implanted medical devices and wounds while resisting drug treatments. Faced with the challenge of *S. epidermidis* resistance, researchers and clinicians urgently need to deepen their understanding of its resistance mechanisms and infection pathways to devise more targeted treatment strategies. However, due to its widespread presence on the human body and its multiple beneficial effects, such as immune modulation, traditional preventive measures against pathogenic infections, such as vaccination or removal of host surface pathogens, are not applicable. Therefore, in-depth research on the resistance and pathogenic mechanisms of *S. epidermidis* fills a gap in understanding its molecular mechanisms, providing theoretical support for the subsequent analysis of clinically resistant strains and the development of antimicrobial drugs, which is crucial for finding new effective drugs and developing new treatment methods.

In recent years, the pathogenicity and antimicrobial resistance of *S. epidermidis* have garnered increasing attention, presenting substantial challenges for infection control within healthcare settings. Genomic analyses conducted in our study have identified genes linked to virulence factors, antibiotic resistance, and cationic antimicrobial peptide (CAMP) resistance among the isolated *S. epidermidis* strains. The presence of these genes suggests the potential pathogenicity and antibiotic resistance of this bacterial strain. Consequently, future research and clinical efforts should focus on a deeper understanding of the genetic profiles of *S. epidermidis* to better mitigate the associated health risks, decrease the prevalence of nosocomial infections, and safeguard the well-being of both patients and healthcare personnel.

Conclusion

This study reveals critical insights into the multidrug-resistant *Staphylococcus epidermidis* HE23 strain isolated from neonatal incubators. Genomic and metabolomic analyses demonstrated that *S. epidermidis* HE23 harbors a chromosome and two plasmids encoding nine antibiotic resistance genes,

including *blaZ*, *mecA*, and the plasmid-borne *mupA*, conferring resistance to β-lactams and quinolones. Metabolomic profiling identified toxic secondary metabolites (cinobufagin, harmaline) with potential implications for neonatal infection severity. Comparative genomic analysis highlighted high similarity to reference strains (ANI >99.3%), yet unique genomic rearrangements and 15 strain-specific protein clusters linked to multidrug efflux systems suggest adaptive evolution under clinical selection pressures. Notably, this is the first report of plasmid-mediated *mupA* coexisting with chromosomal β-lactam resistance genes (*blaZ*/*mecA*) in incubator-derived *S. epidermidis*, underscoring its role as a reservoir for horizontal resistance gene transfer. Future studies should prioritize elucidating *mupA*'s transmission dynamics and synergistic interactions between biofilm formation and metabolite toxicity in neonatal pathogenesis. These investigations will guide targeted strategies to mitigate multidrug-resistant infections in NICUs.

Declarations

Data availability statement

The raw whole-genome sequencing data of *S. epidermidis* HE23, comprising one chromosome (GenBank accession number: CP178841) and two plasmids (GenBank accession numbers: CP178842 and CP178843), are available under NCBI BioProject PRJNA1213267 and BioSample SAMN46322580. The raw metabolomics data and processed results have been deposited in the Metabolomics Workbench (Project ID: PR002355; DOI: 10.21228/M8753X).

Conflict of interest statement

The authors declare that they have no known competing financial interests or personal relationships that could influence the work reported in this paper.

Funding Declaration

This work was partially supported by National Natural Science Foundation of China (No. 81974306), the Research Fund of the Anhui Institute of Translational Medicine (2025zh-03), the National Natural Science Foundation of China (No. 81974306), Anhui Provincial Natural Science Foundation (2208085QH231), the Natural Science Foundation in Higher Education of Anhui (KJ2021A0244).

References

1. M. Reboux, M. Chavignon, A. Tristan, F. Plaisant, F. Laurent, M. Butin, Disinfection of incubators in neonatal intensive care units: impact of steam pulverization on bacterial colonization, Antimicrobial Resistance & Infection Control 12(1) (2023) 18.
2. N.A. Turner, D.J. Anderson, Hospital Infection Control: Clostridioides difficile, Clinics in colon and rectal surgery 33(2) (2020) 98-108.

3. C.J. Donskey, Beyond high-touch surfaces: Portable equipment and floors as potential sources of transmission of health care-associated pathogens, American journal of infection control 47s (2019) A90-a95.
4. H.A. Khan, F.K. Baig, R. Mehboob, Nosocomial infections: Epidemiology, prevention, control and surveillance, Asian Pacific Journal of Tropical Biomedicine 7(5) (2017) 478-482.
5. M. Fattorini, G. Buonocore, D. Lenzi, S. Burgassi, R.M.R. Cardaci, K.P. Biermann, G. Cevenini, G. Messina, Public Health since the beginning: Neonatal incubators safety in a clinical setting, Journal of Infection and Public Health 11(6) (2018) 788-792.
6. M. Chavignon, M. Reboux, J. Tasse, A. Tristan, O. Claris, F. Laurent, M. Butin, Persistent microbial contamination of incubators despite disinfection, Pediatric research 90(6) (2021) 1215-1220.
7. L.E. Hartz, W. Bradshaw, D.H. Brandon, Potential NICU Environmental Influences on the Neonate's Microbiome: A Systematic Review, Advances in Neonatal Care 15(5) (2015) 324-35.
8. K.E. Gregory, Microbiome aspects of perinatal and neonatal health, The Journal of perinatal & neonatal nursing 25(2) (2011) 158-62; quiz 163-4.
9. O. Ozdemir, Primary immunodeficiency diseases in the newborn, Northern Clinics of Istanbul (2536-4553 (Electronic)).
10. T. Oranges, V. Dini, M. Romanelli, Skin Physiology of the Neonate and Infant: Clinical Implications, Advances in wound care (New Rochelle) 4(10) (2015) 587-595.
11. J.M. Melville, T.J. Moss, The immune consequences of preterm birth, Frontiers in neuroscience 7 (2013) 79.
12. M.M. Severn, A.R. Horswill, Staphylococcus epidermidis and its dual lifestyle in skin health and infection, Nature Reviews Microbiology 21(2) (2023) 97-111.
13. C. Leonel, I.F.G. Sena, W.N. Silva, P. Prazeres, G.R. Fernandes, P. Mancha Agresti, M. Martins Drumond, A. Mintz, V.A.C. Azevedo, A. Birbrair, Staphylococcus epidermidis role in the skin microenvironment, Journal of cellular and molecular medicine 23(9) (2019) 5949-5955.
14. M. Otto, Staphylococcus epidermidis--the 'accidental' pathogen, Nature Reviews Microbiology 7(8) (2009) 555-67.
15. M.M. Brown, A.R. Horswill, Staphylococcus epidermidis-Skin friend or foe?, PLoS pathogens 16(11) (2020) e1009026.
16. S.M.K. Schoenfelder, C. Lange, M. Eckart, S. Hennig, S. Kozytska, W. Ziebuhr, Success through diversity – How Staphylococcus epidermidis establishes as a nosocomial pathogen, International Journal of Medical Microbiology 300(6) (2010) 380-386.
17. S. Hogan, N.T. Stevens, H. Humphreys, J.P. O'Gara, E. O'Neill, Current and future approaches to the prevention and treatment of staphylococcal medical device-related infections, Current pharmaceutical design 21(1) (2015) 100-13.
18. A. Farajzadeh Sheikh, A. Asareh Zadegan Dezfuli, T. Navidifar, S.S. Fard, M. Dehdashtian, Association between biofilm formation, structure and antibiotic resistance in Staphylococcus epidermidis

isolated from neonatal septicemia in southwest Iran, Infection and drug resistance 12 (2019) 1771-1782.

19. M.U. Akbar, A. Haque, S. Liaquat, P. Schierack, A. Ali, Biofilm Formation by Staphylococcus epidermidis and Its Inhibition Using Carvacrol, 2-Aminobenzemidazole, and 3-Indole Acetonitrile, ACS Omega 8(1) (2023) 682-687.
20. I.A. Joubert, M. Otto, T. Strunk, A.J. Currie, Look Who's Talking: Host and Pathogen Drivers of Staphylococcus epidermidis Virulence in Neonatal Sepsis, International journal of molecular sciences 23(2) (2022).
21. S. Chen, Y. Zhou, Y. Chen, J. Gu, fastp: an ultra-fast all-in-one FASTQ preprocessor, Bioinformatics (Oxford, England) 34(17) (2018) i884-i890.
22. R.R. Wick, L.M. Judd, C.L. Gorrie, K.E. Holt, Unicycler: Resolving bacterial genome assemblies from short and long sequencing reads, PLoS computational biology 13(6) (2017) e1005595.
23. A. Gurevich, V. Saveliev, N. Vyahhi, G. Tesler, QUAST: quality assessment tool for genome assemblies, Bioinformatics (Oxford, England) 29(8) (2013) 1072-5.
24. T. Seemann, Prokka: rapid prokaryotic genome annotation, Bioinformatics (Oxford, England) 30(14) (2014) 2068-9.
25. D. Hyatt, G.L. Chen, P.F. Locascio, M.L. Land, F.W. Larimer, L.J. Hauser, Prodigal: prokaryotic gene recognition and translation initiation site identification, BMC bioinformatics 11 (2010) 119.
26. B. Buchfink, C. Xie, D.H. Huson, Fast and sensitive protein alignment using DIAMOND, Nature Methods 12(1) (2015) 59-60.
27. B. Liu, D. Zheng, S. Zhou, L. Chen, J. Yang, VFDB 2022: a general classification scheme for bacterial virulence factors, Nucleic acids research 50(D1) (2022) D912-d917.
28. X. Yin, X.T. Jiang, B. Chai, L. Li, Y. Yang, J.R. Cole, J.M. Tiedje, T. Zhang, ARGs-OAP v2.0 with an expanded SARG database and Hidden Markov Models for enhancement characterization and quantification of antibiotic resistance genes in environmental metagenomes, Bioinformatics 34(13) (2018) 2263-2270.
29. Z. Zhou, P.Q. Tran, A.M. Breister, Y. Liu, K. Kieft, E.S. Cowley, U. Karaoz, K. Anantharaman, METABOLIC: high-throughput profiling of microbial genomes for functional traits, metabolism, biogeochemistry, and community-scale functional networks, Microbiome 10(1) (2022) 33.
30. Microbial metabolite harmaline protects against virus-induced systemic inflammation, Nature Microbiology 8(1) (2023) 10-11.
31. K. Blin, S. Shaw, H.E. Augustijn, Z.L. Reitz, F. Biermann, M. Alanjary, A. Fetter, B.R. Terlouw, W.W. Metcalf, E.J.N. Helfrich, G.P. van Wezel, M.H. Medema, T. Weber, antiSMASH 7.0: new and improved predictions for detection, regulation, chemical structures and visualisation, Nucleic acids research 51(W1) (2023) W46-w50.
32. X.Y. Zheng, Z.J. Zhang, G.X. Chou, T. Wu, X.M. Cheng, C.H. Wang, Z.T. Wang, Acetylcholinesterase inhibitive activity-guided isolation of two new alkaloids from seeds of Peganum nigellastrum Bunge by an in vitro TLC- bioautographic assay, Archives of pharmacal research 32(9) (2009) 1245-51.

33. C.L. Dai, R.J. Zhang, P. An, Y.Q. Deng, K. Rahman, H. Zhang, Cinobufagin: a promising therapeutic agent for cancer, Journal of Pharmacy and Pharmacology 75(9) (2023) 1141-1153.
34. H. Zhang, B. Jian, H. Kuang, Pharmacological Effects of Cinobufagin, Medical Science Monitor 29 (2023) e940889.
35. P. Seguinot, A. Ortiz-Julien, C. Camarasa, Impact of Nutrient Availability on the Fermentation and Production of Aroma Compounds Under Sequential Inoculation With M. pulcherrima and S. cerevisiae, Frontiers in microbiology 11 (2020) 305.
36. H.C. Flemming, J. Wingender, U. Szewzyk, P. Steinberg, S.A. Rice, S. Kjelleberg, Biofilms: an emergent form of bacterial life, Nature reviews. Microbiology 14(9) (2016) 563-75.
37. J.L. Anaya-López, J.E. López-Meza, A. Ochoa-Zarzosa, Bacterial resistance to cationic antimicrobial peptides, Critical Reviews in Microbiology 39(2) (2013) 180-195.
38. W. Zhou, M. Spoto, R. Hardy, C. Guan, E. Fleming, P.J. Larson, J.S. Brown, J. Oh, Host-Specific Evolutionary and Transmission Dynamics Shape the Functional Diversification of Staphylococcus epidermidis in Human Skin, Cell 180(3) (2020) 454-470.e18.
39. M. Sabaté Brescó, L.G. Harris, K. Thompson, B. Stanic, M. Morgenstern, L. O'Mahony, R.G. Richards, T.F. Moriarty, Pathogenic Mechanisms and Host Interactions in Staphylococcus epidermidis Device-Related Infection, Frontiers in microbiology 8 (2017) 1401.
40. S. Kleinschmidt, F. Huygens, J. Faoagali, I.U. Rathnayake, L.M. Hafner, Staphylococcus epidermidis as a cause of bacteremia, Future microbiology 10(11) (2015) 1859-79.
41. H. Büttner, D. Mack, H. Rohde, Structural basis of Staphylococcus epidermidis biofilm formation: mechanisms and molecular interactions, Frontiers in cellular and infection microbiology 5 (2015) 14.
42. I.A. Joubert, M. Otto, T. Strunk, A.J. Currie, Look Who's Talking: Host and Pathogen Drivers of Staphylococcus epidermidis Virulence in Neonatal Sepsis, International journal of molecular sciences 23(2) (2022).
43. S.A. Coggins, K. Glaser, Updates in Late-Onset Sepsis: Risk Assessment, Therapy, and Outcomes, NeoReviews 23(11) (2022) 738-755.
44. N.S. Boghossian, G.P. Page, E.F. Bell, B.J. Stoll, J.C. Murray, C.M. Cotten, S. Shankaran, M.C. Walsh, A.R. Laptook, N.S. Newman, E.C. Hale, S.A. McDonald, A. Das, R.D. Higgins, Late-onset sepsis in very low birth weight infants from singleton and multiple-gestation births, The Journal of pediatrics 162(6) (2013) 1120-4, 1124.e1.
45. B.J. Stoll, N. Hansen, A.A. Fanaroff, L.L. Wright, W.A. Carlo, R.A. Ehrenkranz, J.A. Lemons, E.F. Donovan, A.R. Stark, J.E. Tyson, W. Oh, C.R. Bauer, S.B. Korones, S. Shankaran, A.R. Laptook, D.K. Stevenson, L.A. Papile, W.K. Poole, Late-onset sepsis in very low birth weight neonates: the experience of the NICHD Neonatal Research Network, Pediatrics 110(2 Pt 1) (2002) 285-91.
46. Y. Dong, C.P. Speer, K. Glaser, Beyond sepsis: Staphylococcus epidermidis is an underestimated but significant contributor to neonatal morbidity, Virulence 9(1) (2018) 621-633.

47. B.A. Shah, J.F. Padbury, Neonatal sepsis: an old problem with new insights, Virulence 5(1) (2014) 170-8.
48. Y. Dong, C.P. Speer, Late-onset neonatal sepsis: recent developments, Archives of disease in childhood. Fetal and neonatal edition 100(3) (2015) F257-63.
49. L. Fišarová, T. Botka, X. Du, I. Mašlaňová, P. Bárdy, R. Pantůček, M. Benešík, P. Roudnický, V. Winstel, J. Larsen, R. Rosenstein, A. Peschel, J. Doškař, Staphylococcus epidermidis Phages Transduce Antimicrobial Resistance Plasmids and Mobilize Chromosomal Islands, mSphere 6(3) (2021).
50. J.F. Fisher, S. Mobashery, β-Lactam Resistance Mechanisms: Gram-Positive Bacteria and Mycobacterium tuberculosis, Cold Spring Harbor perspectives in medicine 6(5) (2016).
51. H. Lade, J.S. Kim, Molecular Determinants of β-Lactam Resistance in Methicillin-Resistant Staphylococcus aureus (MRSA): An Updated Review, Antibiotics (Basel, Switzerland) 12(9) (2023).
52. J. Rolo, P. Worning, J. Boye Nielsen, R. Sobral, R. Bowden, O. Bouchami, P. Damborg, L. Guardabassi, V. Perreten, H. Westh, A. Tomasz, H. de Lencastre, M. Miragaia, Evidence for the evolutionary steps leading to mecA-mediated β-lactam resistance in staphylococci, PLOS Genetics 13(4) (2017) e1006674.
53. S. Schwendener, V. Perreten, The bla and mec families of β-lactam resistance genes in the genera Macrococcus, Mammaliicoccus and Staphylococcus: an in-depth analysis with emphasis on Macrococcus, Journal of Antimicrobial Chemotherapy 77(7) (2022) 1796-1827.
54. E.R. Holden, M. Yasir, A.K. Turner, I.G. Charles, M.A. Webber, Tazobactam selects for multidrug resistance, npj Antimicrobials and Resistance 3(1) (2025) 48.
55. C. Reading, M. Cole, Clavulanic acid: a beta-lactamase-inhiting beta-lactam from Streptomyces clavuligerus, Antimicrobial agents and chemotherapy 11(5) (1977) 852-7.
56. Y. Wang, X. Shi, J. Zhang, Y. Wang, Y. Lv, X. Du, Q. ChaoLuMen, J. Wang, Wide spread and diversity of mutation in the gyrA gene of quinolone-resistant Corynebacterium striatum strains isolated from three tertiary hospitals in China, Annals of clinical microbiology and antimicrobials 20(1) (2021) 71.
57. J.N. Ramos, T.B. Valadão, P.V.P. Baio, A.L. Mattos-Guaraldi, V.V. Vieira, Novel mutations in the QRDR region gyrA gene in multidrug-resistance Corynebacterium spp. isolates from intravenous sites, Antonie van Leeuwenhoek 113(4) (2020) 589-592.
58. M.J. Walker, R.G. Birch, J.M. Pemberton, Cloning and characterization of an albicidin resistance gene from Klebsiella oxytoca, Molecular microbiology 2(4) (1988) 443-54.
59. A.S. Lee, H. de Lencastre, J. Garau, J. Kluytmans, S. Malhotra-Kumar, A. Peschel, S. Harbarth, Methicillin-resistant Staphylococcus aureus, Nature Reviews Disease Primers 4(1) (2018) 18033.
60. I.E. Mba, E.I. Nweze, Antimicrobial Peptides Therapy: An Emerging Alternative for Treating Drug-Resistant Bacteria, Yale Journal of Biology and Medicine 95(4) (2022) 445-463.
61. D.J. Diekema, M.A. Pfaller, F.J. Schmitz, J. Smayevsky, J. Bell, R.N. Jones, M. Beach, Survey of infections due to Staphylococcus species: frequency of occurrence and antimicrobial susceptibility of isolates collected in the United States, Canada, Latin America, Europe, and the Western Pacific

region for the SENTRY Antimicrobial Surveillance Program, 1997-1999, Clinical Infectious Diseases 32 Suppl 2 (2001) S114-32.

62. L. Yang, W. Jing, Q. Jian, N. Rui, D. Bao, Clinical Distribution and Antimicrobial Resistance Analysis of Staphylococcus epidermidis Laboratory Medicine and Clinical Practice 20(17) (2023) 2599-2602.

Figures

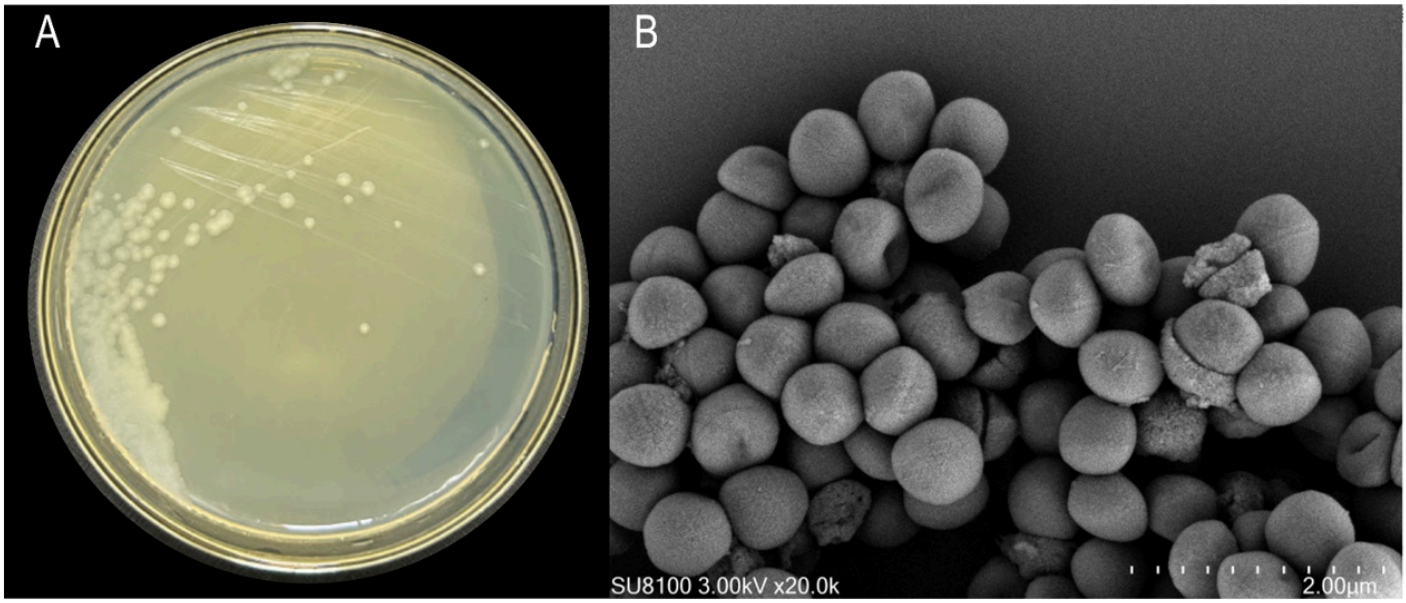


Figure 1

Morphological characterization of *S. epidermidis* HE23. (**A**) Colony morphology on agar plates after 24-hour incubation. (**B**) Scanning electron micrograph of *S. epidermidis* HE23 (SU8100 microscope, 3.00 kV acceleration voltage, ×20,000 magnification; scale bar: 2.00 µm).

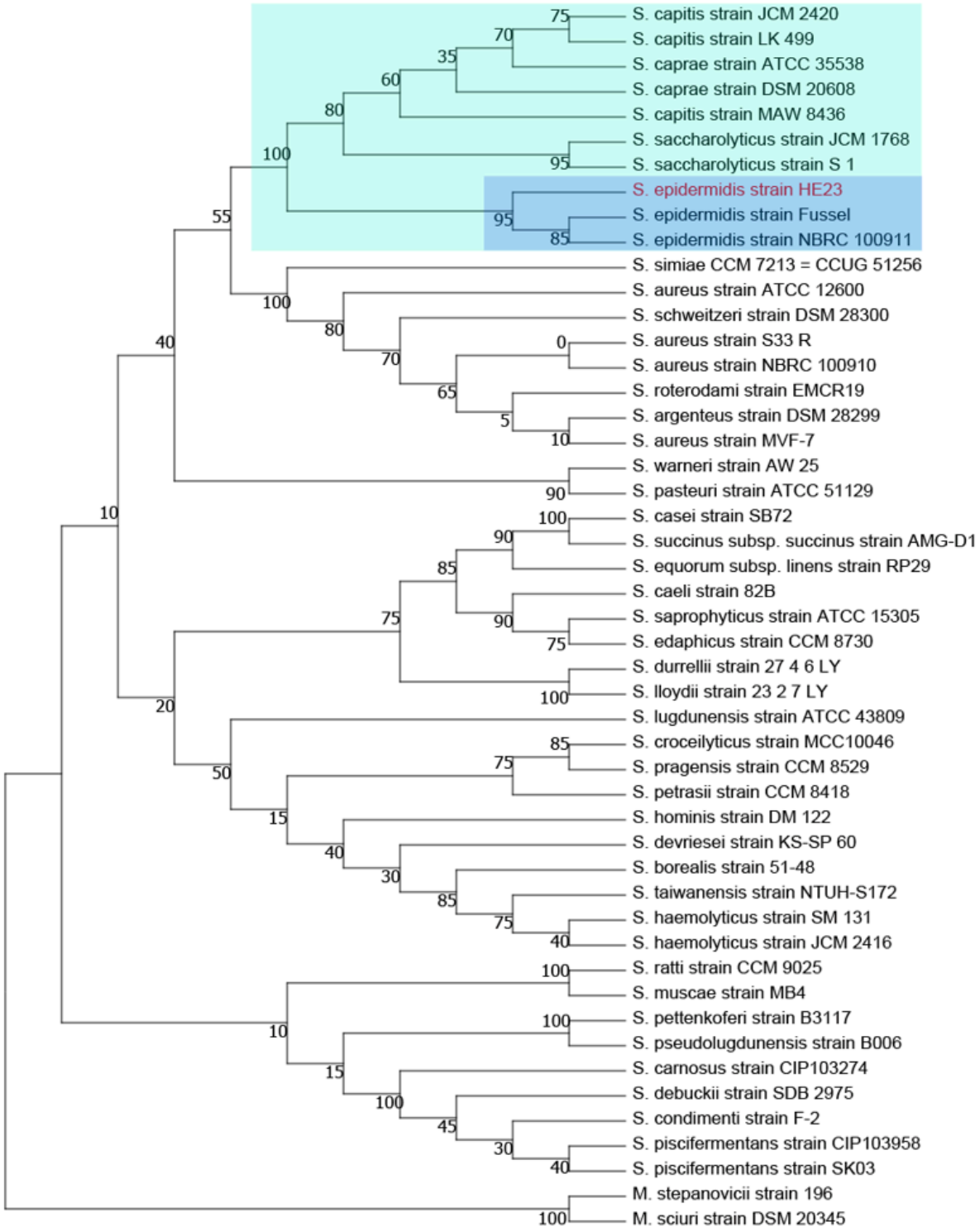


Figure 2

Phylogenetic tree constructed based on the 16S rRNA gene sequences of *S. epidermidis* HE23 and other related strains. The tree was built using the Maximum Likelihood method, and the support for each node was assessed through Bootstrap analysis (1000 replicates). The numbers on the branches indicate the Bootstrap support values (percentages).

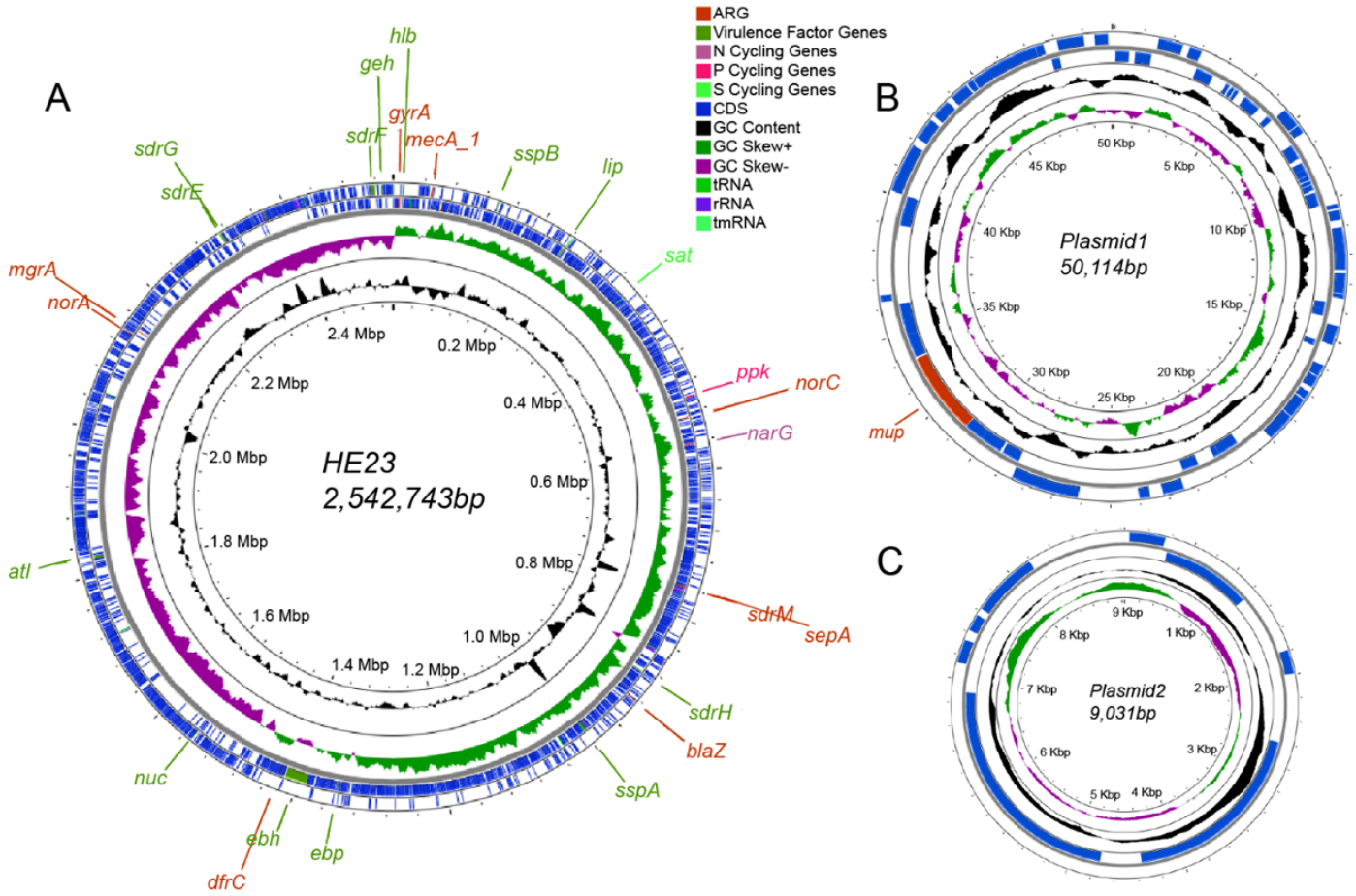


Figure 3

Functional annotations for S. epidermidis HE23. (**A**) The chromosomal circular map illustrates the core genome structure of *S. epidermidis* HE23 . The map displays the key functional regions of the genome in an inner-to-outer sequence: the innermost circle represents the genome length scale, the middle region shows GC content and GC skew, and the outer circle indicates annotated gene positions with some important genes marked. (**B**) The functional annotation of Plasmid 1 was visualized and it harbors antibiotic resistance genes. (**C**) The functional annotation of Plasmid 2 was visualized.

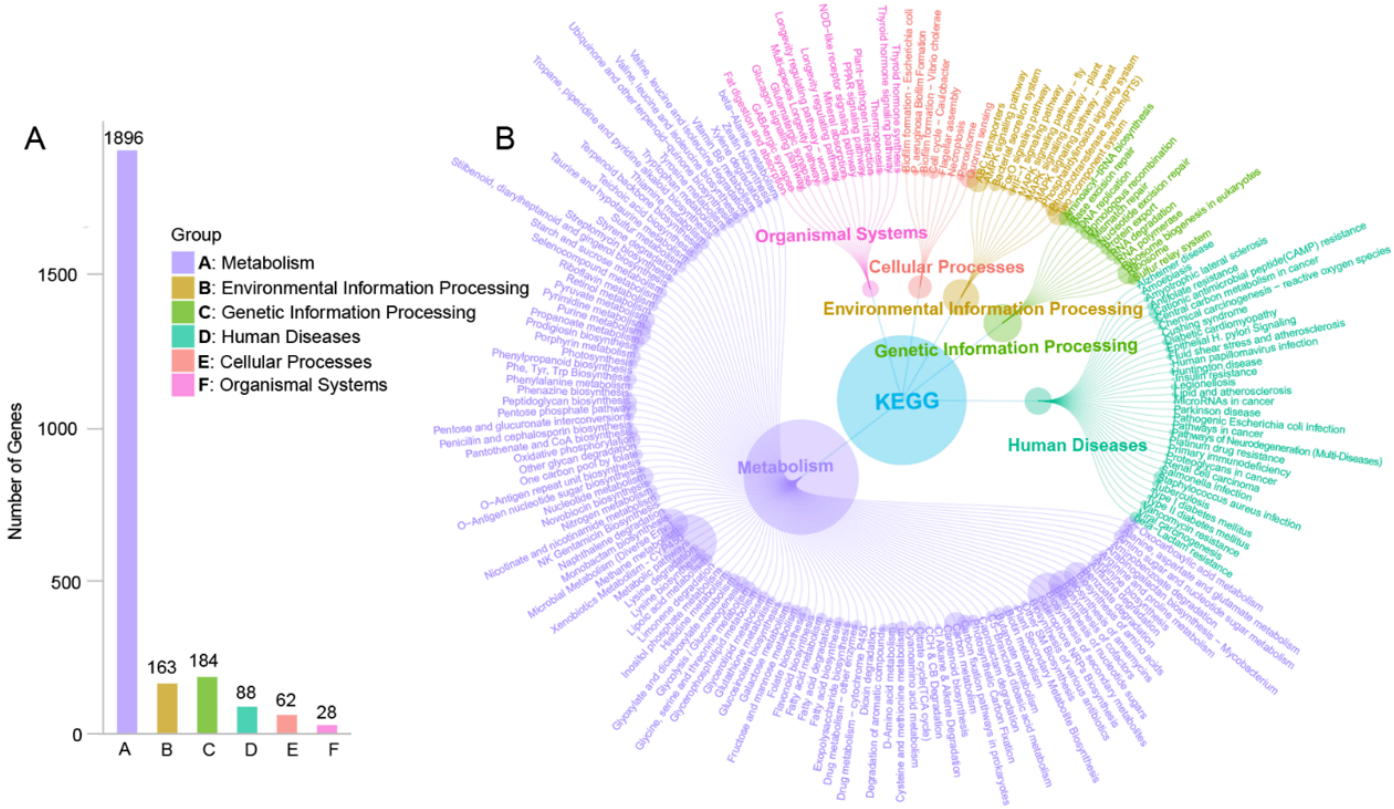


Figure 4

KEGG metabolic pathway visualization of *S. epidermidis* HE23 whole genome. (**A**) Gene distribution of KEGG metabolic pathways in the *S. epidermidis* HE23 genome. (**B**) KEGG metabolic pathway network in *S. epidermidis* HE23.

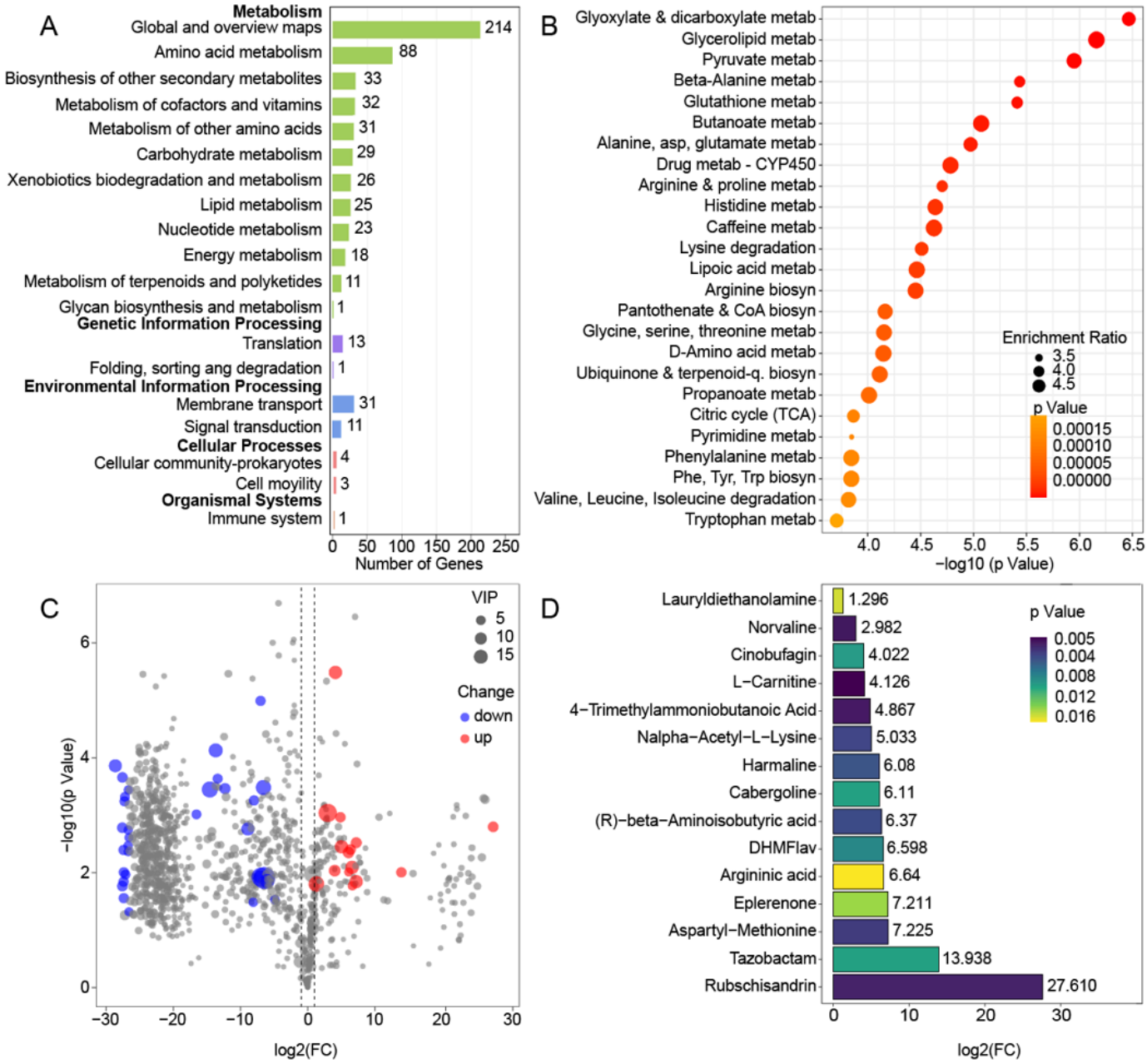


Figure 5

Metabolic Features and Diûerential Metabolites of *S. epidermidis* HE23. (**A**) Gene distribution of metabolic pathways in *S. epidermidis* HE23 . (**B**) Top 25 enriched metabolic pathways in *S. epidermidis* HE23. (**C**) Volcano plot of diûerential metabolites in *S. epidermidis* HE23 . (**D**) Relative abundance changes of upregulated diûerential metabolites in *S. epidermidis* HE23 .

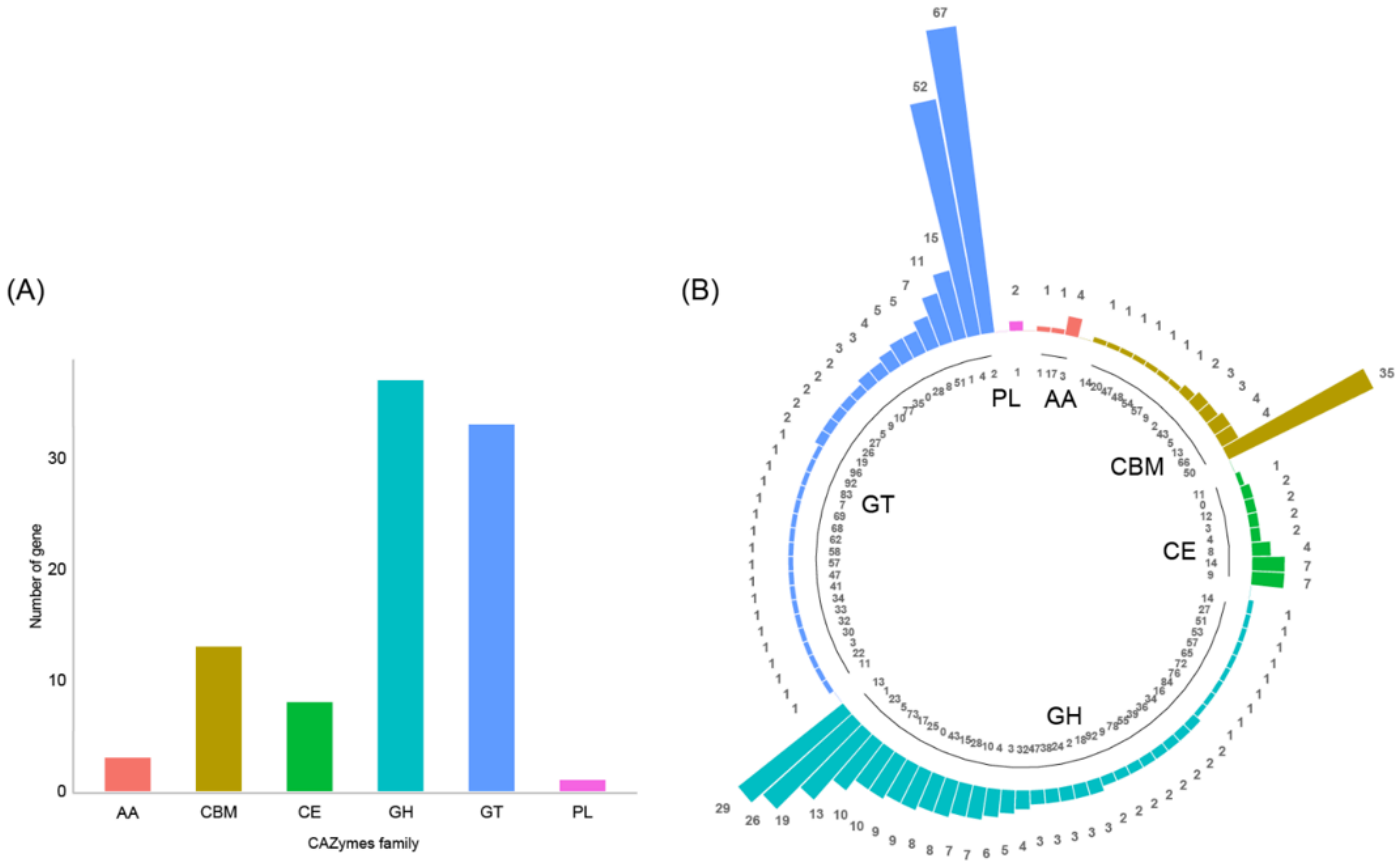


Figure 6

CAZymes in *S. epidermidis* HE23. (**A**) Number of CAZymes and their relevant family. (**B**) CAZymes family distribution. Numbers near the internal circle and at the top of the bars represent the family ID and the number of proteins, respectively. AA: auxiliary activity, CBM: carbohydrate-binding module, CE: carbohydrate esterase, GH: glycoside hydrolase, GT: glycosyl transferase, PL: polysaccharide lyase.

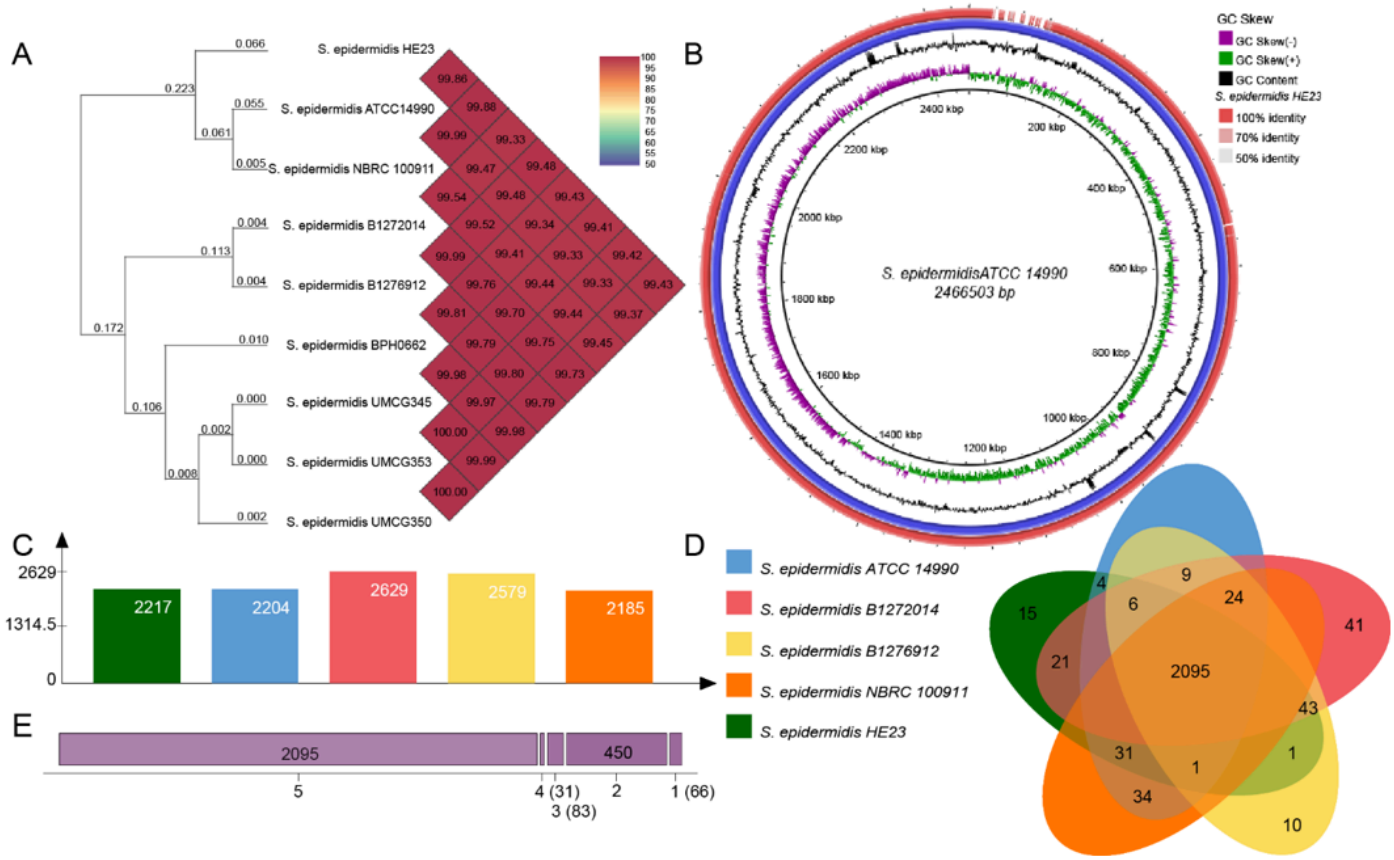


Figure 7

Comparative genomic analysis of *S. epidermidis* HE23. (**A**) Phylogenetic heatmap based on OrthoANI values between *S. epidermidis* HE23 and related strains. (**B**) Circular genome comparison map between *S. epidermidis* HE23 and *S. epidermidis*ATCC 14990. (**C**) Bar chart comparing total protein counts across five *S. epidermidis* strains. (**D**) The distribution of shared and unique protein clusters among the five strains. (**E**) Proportional distribution of conserved versus strain-specific protein clusters across the five strains.